Journal of Chromatography A, 1241 (2012) 69–75

Contents lists available at SciVerse ScienceDirect

Journal of Chromatography A

journal homepage: www.elsevier.com/locate/chroma

The obstruction factor in size-exclusion chromatography. 2. The interparticle, intraparticle, and total obstruction factors

Dustin J. Richard [a], André M. Striegel [b,*]

[a] Department of Chemistry & Biochemistry, Florida State University, Tallahassee, FL 32306, USA
[b] Analytical Chemistry Division, National Institute of Standards and Technology, 100 Bureau Drive, Mail Stop 8392, Gaithersburg, MD 20899, USA

ARTICLE INFO

Article history:
Received 3 February 2012
Received in revised form 5 April 2012
Accepted 8 April 2012
Available online 17 April 2012

Keywords:
Size-exclusion chromatography
Obstruction factor
Band broadening
Hydrodynamic chromatography

ABSTRACT

"Obstruction factor" is a generic rubric under which are usually gathered the interparticle, intraparticle, stationary phase, and total obstruction factors, γ_e, γ_p, γ_s, and γ_t, respectively. These, in turn, affect longitudinal diffusion and stationary, mobile phase, and stagnant mobile phase mass transfer. We conclude here our investigation into the various obstruction factors operative in size-exclusion chromatography (SEC). Stop-flow experiments were employed to determine either the interparticle (for analytes with $K_{SEC} = 0$) or the total (for analytes with $K_{SEC} > 0$) obstruction factor, and these results were combined with those from variable-flow-rate experiments which provided the intraparticle obstruction factor. Because of minimal enthalpic interactions between the analytes and stationary phase, in SEC $\gamma_s \approx 0$, which allows for isolation of the other obstruction factors. A relationship between γ_t, γ_e, and γ_p was proposed for SEC, based on previous independent work and dependent upon the various column porosities. This relationship was extended to hydrodynamic chromatography, a technique in which, ideally, both γ_s and γ_p are equal to zero.

Published by Elsevier B.V.

1. Introduction

Band broadening adversely affects all forms of chromatography. In so-called "small molecule" enthalpically driven separations, it limits the number of peaks that can be unambiguously discriminated from each other, i.e., the peak capacity of the system. In macromolecular entropically driven techniques, band broadening manifests itself more noticeably by how it affects the molar mass (M) averages and the molar mass distribution (MMD) determined when employing, most especially but not exclusively, peak-position calibration curves. As such, an improved understanding of band broadening can enhance the power of the former methods and the accuracy of the latter.

When discussing band broadening, it is not unusual to encounter mention of the column obstruction factor γ. This factor denotes the hindered diffusion of solute within a packed column (D_{eff}), as compared to the unobstructed diffusion of the same solute in an open tube (D_m), as per:

$$\gamma = \frac{D_{eff}}{D_m} \tag{1}$$

The ubiquity of γ in the literature is matched only by the short shrift it is usually given in the accompanying discussions, where it is perfunctorily mentioned that the obstruction factor affects longitudinal (B-term) diffusion and that γ has a constant value of approximately 0.6. Statements like this one fail to distinguish among the total, interparticle, intraparticle, and stationary phase obstruction factors (γ_t, γ_e, γ_p, and γ_s, respectively). They also take into account only the γ_e term, which affects B-term diffusion, not the γ_p term, which affects intraparticle or stagnant mobile phase mass transfer (C_{SM} term in the expanded van Deemter equation), nor the γ_s term, which affects mass transfer in the stationary phase (C_S term) of so-called "interactive" (i.e., enthalpically dominated) liquid chromatography (LC) separations.

In his classic *Dynamics of Chromatography* [1], Giddings noted that the value of γ (actually, of γ_e) of 0.60 ± 0.02 determined by Knox and McLaren using gas chromatography (GC) columns packed with glass beads [2] is close to the theoretical value of 0.63 and likely to be a good approximation when using most nonporous, densely packed granular materials in both LC and GC. Giddings also mentioned that, when all types of chromatographic materials are taken into account, the range spanned by γ_e appears to be between 0.4 and 0.9 (for all γ, higher values correspond to less obstruction to diffusion, and vice versa). He postulated that this is also likely to be the range spanned by γ_p, and that a reasonable value for γ_s is approximately 0.5. Other hypotheses of Giddings regarding the various γ included his prediction that γ_e is likely to be

* Corresponding author. Tel.: +1 301 975 3159; fax: +1 301 977 0685.
E-mail address: andre.striegel@nist.gov (A.M. Striegel).

0021-9673/$ – see front matter. Published by Elsevier B.V.
http://dx.doi.org/10.1016/j.chroma.2012.04.024

flow-rate-dependent and to increase in magnitude with increasing reduced velocity, that $\gamma_s \ll 0.5$ may be possible for strongly retained materials, and that differences (albeit small, on the order of no more than 0.1) may exist in γ_e in the flow versus lateral direction in non-isotropic media (e.g., in paper chromatography). We note that the predicted flow-rate-dependence of γ_e was later confirmed by Hawkes [3]. However, recent experiments by our group, described below and, more fully, in reference [4], have demonstrated that $\gamma_p \ll 0.4$ seem to be the norm in size-exclusion chromatography (as predicted qualitatively by Knox and Scott in 1983 [5], who noted that $\gamma_p < 0.6$ would be likely when steric exclusion played a significant role in the separation). In addition to the classic work of Knox [2,5–7], to the experiments by Hawkes in the early 1970s [3,8] and by Klein and Grüneberg in the early 1980s [9], and to our own work on γ_p [4], recent research into the obstruction factor includes that from the Miyabe and Bushey groups [10,11], also on γ_p, and of the Guiochon group on both γ_p and γ_e [12–15].

As mentioned above, as part of our exploration of the various γ terms, our group recently demonstrated, using size-exclusion chromatography (SEC) [16], the dependence of the intraparticle obstruction factor γ_p on analyte parameters (molar mass, monomeric repeat unit chemistry), user-controlled variables (flow rate, temperature), and column characteristics (particle size, pore size), individually [4]. Among many other observations we noted that, over a molar mass range of three orders of magnitude, in no case was γ_p observed to exceed 0.2 (and, in most of the polymers studied, was < 0.1), a value well below the lowest γ_p of 0.4 predicted by Giddings. Our approach to measuring γ_p relied on variable-flow-rate experiments and the application of Eq. (2) [1,4,9]:

$$\gamma_p = \frac{K_{SEC} V_i d_p^2}{30\ D_m(\partial\sigma^2_{perm}/\partial u)} \quad (2)$$

where K_{SEC} is the solute distribution coefficient in an SEC experiment, V_i is the internal pore volume of the packed column, d_p is the diameter of the column packing material, D_m is the unobstructed diffusion coefficient of the solute in the mobile phase, and $\partial\sigma^2_{perm}/\partial u$ is the change in peak variance with changing flow rate. Unfortunately, because for totally excluded solutes $K_{SEC} = 0$, this equation is not applicable to determining the interparticle obstruction factor γ_e. For the latter, we employ here the classic stop-flow (also known as peak parking) method of Giddings and Knox, which we had previously used to study B-term diffusion in SEC [17]. In stop-flow experiments, rather than relying on measurements performed using a series of increasing (or decreasing) flow rates, as was done when determining γ_p, we rely rather on injecting the analyte onto the column and letting it travel partway through the column, then abruptly stopping the flow. The analyte is subsequently held on the column at zero flow rate for varying periods of increasing (or decreasing) length, after which the flow rate is abruptly started once again. The change in peak variance as a function of hold time, $\partial\sigma_t^2/\partial t$, is measured, and this datum is then used to calculate γ_e using Eq. (3) [1]:

$$\gamma_\beta = \frac{(\partial\sigma_t^2/\partial t)\nu^2}{2D_m} \quad \text{when } K_{SEC} = 0, \quad \beta = e; \quad \text{when } K_{SEC} > 0, \quad \beta = t \quad (3)$$

where ν is the linear flow velocity of the analyte (see Eq. (6) below). For retained solutes (i.e., those that permeate into the pores of the SEC columns, for which $K_{SEC} > 0$), the obstruction factor determined using Eq. (3) is actually the total obstruction factor γ_t, which includes contributions from both γ_e and γ_p.

Our choice of SEC as a technique for determining the various γ terms is based on a number of factors. First, SEC is an entropically controlled technique, where sorptive interactions are generally negligible (confirmed experimentally for the analytes studied here, as described in Section 2.2 and in Refs. [16,18–20]). This corresponds to $C_S \approx 0$ in the expanded van Deemter equation and, consequently, $\gamma_s \approx 0$ as well. Second, because B-term diffusion is essentially insignificant in SEC for most linear analytes with $M > 30{,}000\ \mathrm{g\,mol^{-1}}$ [17], we did not need to worry about longitudinal diffusion contributions to band broadening when determining γ_p using the variable-flow-rate approach. On the other hand, this negligible B-term diffusion also limits the analytes we can employ for determining γ_e, as we cannot measure $\partial\sigma_t^2/\partial t$ for analytes with M much larger than approximately $30{,}000\ \mathrm{g\,mol^{-1}}$. A narrower M range means that we cannot examine a relatively large number of narrow dispersity, well-characterized standards, as we did in our studies of γ_p. This fact, combined with the extreme length of stop flow experiments, means the number of analytes employed in the present study is rather limited, as compared to the number used in our study of γ_p. As will be seen, however, even using a smaller data set a number of interesting conclusions about γ_t, γ_e, γ_p and their relationships to one another became evident. Issues of band breadth resulting from the molar mass dispersity inherent in all synthetic polymers were dispensed with by employing narrow dispersity standards and by the fact that the contribution to band broadening arising from molar mass dispersity is constant and, therefore, cancels out when measuring the *change* in band broadening as a function of either flow rate or hold time [4,14].

2. Experimental

2.1. Materials

Tetrahydrofuran (THF), spectrophotometric grade, inhibited with 250 ppm butylated hydroxytoluene, was purchased from J.T. Baker (Philipsburg, NJ, USA), and toluene was purchased from Fisher Scientific (Fair Lawn, NJ, USA). Narrow dispersity ($M_w/M_n \leq 1.03$) polystyrene (PS) standards were purchased from Agilent/Polymer Laboratories (Amherst, MA, USA).

2.2. Chromatography

Each experiment was performed using $1\ \mathrm{mg\,mL^{-1}}$ solutions of PS, a concentration much lower than the critical overlap concentration of even the highest-M PS studied [4]. After adding the polymer to the solvent vials, the latter were shaken gently by hand and the solutions were allowed to solvate overnight. To each vial was added 5 μL of toluene, to determine the total permeation volume of the columns, to act as a flow rate marker, and to provide an additional data point in our studies (see Fig. 1).

Stop-flow SEC experiments were conducted using two styrene/divinylbenzene 300 mm × 7.5 mm columns (both from Agilent/Polymer Laboratories, Amherst, MA, USA), individually: a nominally 5 μm particle size, 50 Å pore size column and a nominally 5 μm particle size, 10^4 Å pore size column. Information provided by the manufacturer indicated that the actual average particle size of these columns was 4 μm, however, which was the particle size used in all calculations and the particle size to which we shall refer throughout this paper. The total exclusion volume of the columns was determined using several high-M polystyrenes which did not penetrate the pores of the columns packing material.

For the 4 μm, 10^4 Å column, the total exclusion volume V_o was 4.510 mL, the empty column volume V_c was 13.254 mL, and the total permeation (void) volume V_M was 9.831 mL. For the 4 μm, 50 Å column, V_o = 5.100 mL, V_c = 13.254 mL, and V_M = 8.209 mL.

100 μL of each sample was injected onto each column using a Waters 2695 Separations Module (Waters, Milford, MA, USA) with on-line degasser and in-line preinjection filter. Samples were allowed to elute for 2 min at $1\ \mathrm{mL\,min^{-1}}$, after which time flow was halted for a given hold time before resuming flow at $1\ \mathrm{mL\,min^{-1}}$.

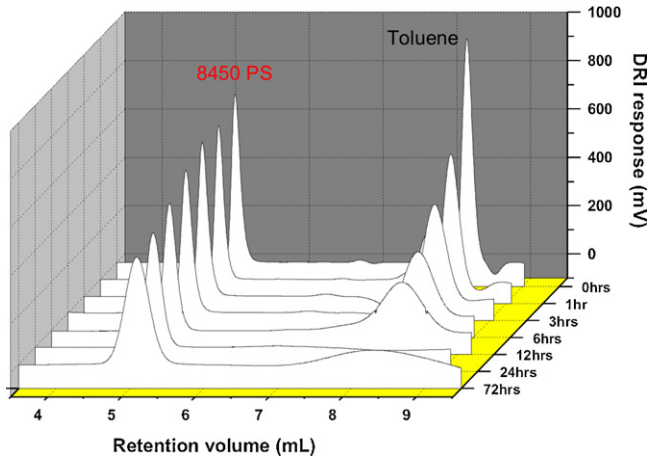

Fig. 1. Overlay of stop-flow chromatograms, as monitored by the differential refractometer (DRI), of solution of PS 8450 with added toluene in 4 μm particle size, 50 Å pore size column. (Note that toluene was not added to the 24 h stop-flow time sample of PS 8450, to demonstrate the negligible influence of the solvent; see Fig. 2, legend.) Solvent: THF, temperature: 30 °C.

Hold times were 1, 3, 6, 12, 24, and 72 h. Detection was performed using an Optilab rEX differential refractometer (Wyatt Technology Corp., Santa Barbara, CA, USA). Each analysis was performed at least in triplicate. All experiments were conducted in THF at 30 ± 1 °C. Select non-stop-flow experiments at 50 °C showed differences in K_{SEC} as a function of temperature 1–2% only, demonstrating that the analytes eluted by a near-ideal size-exclusion mechanism, in the virtual absence of enthalpic interactions.

Data acquisition was performed with Clarity software (version 2.4.1.91) from DataApex (Prague, Czech Republic), determination of peak variances with the Origin Peak Fitting Module (v. 1.4) from OriginLab (Northampton, MA, USA). For simplicity, a Gaussian fit was employed to determine all peak variances, because differences between it and an exponentially modified Gaussian fit were less than 5%, usually substantially so.

3. Results and discussion

Results from our experiments are shown in Table 1 and Figs. 1–4. As can be observed in the figures, the breadth of the chromatographic bands increases with increasing hold time on column (increasing stop-flow time). This is reflected in the linear increase in peak variance with increasing stop-flow time, shown in Figs. 5 and 6. The larger variances in the 10^4 Å column, as compared to those in the 50 Å column, are due to a greater contribution to brand broadening from stagnant mobile phase mass transfer (C_{SM}) effects in the former column as compared to the latter.

Intraparticle obstruction factors were calculated using Eq. (2), the procedure described in Ref. [4], and the recent D_m versus M relationship for PS in THF at 25 °C obtained from [21]:

$$D_m = (2.4 \pm 0.1) \times 10^{-4} M^{(-0.54 \pm 0.01)} \quad (4)$$

after adjusting for differences in temperature (25 versus 30 °C) through the relationship [22]:

$$D_{m,\mathrm{exp}} = D_{m,ref} \left(\frac{T_{\mathrm{exp}}}{T_{ref}} \right) \left(\frac{\eta_{ref}}{\eta_{\mathrm{exp}}} \right) \quad (5)$$

where $D_{m,\mathrm{exp}}$ were the values used in our calculations at an absolute temperature (in Kelvin) T_{exp} in a solvent of viscosity η_{exp}, and comparison was with the D_m values from the literature ($D_{m,ref}$) obtained at an absolute temperature T_{ref} in a solvent of viscosity η_{ref}. For an analyte of a given size (hydrodynamic radius), the constancy of the factor $D_m\eta/T$ is given by the Stokes–Einstein relation (cf. Eq. (12)).

Table 1
Interparticle, intraparticle, and total column obstruction factors and porosities.[a]

Analyte	Obstruction factors[b]				Porosities[b,c]					
	γ_e (50 Å)	γ_t (50 Å)	γ_t (10^4 Å)	γ_p (10^4 Å)	ε_e (50 Å)[d]	ε_t (50 Å)[e]	ε_p (50 Å)[f]	ε_e (10^4 Å)[d]	ε_t (10^4 Å)[e]	ε_p (10^4 Å)[f]
Toluene	–	0.414 ± 0.058	0.602 ± 0.082	–	0.385	0.619	0.381	0.340	0.742	0.608
PS 8450	0.710 ± 0.034	0.442 ± 0.021[g]	0.667 ± 0.030	0.052 ± 0.002[h]	0.385	0.619	0	0.340	0.742	0.406
PS 19,760	–	–	0.740 ± 0.035	0.074 ± 0.004	0.385[i]	0.619[i]	0[i]	0.340	0.742	0.317
PS 31,420	0.717 ± 0.039	0.446 ± 0.024[g]	0.627 ± 0.030	0.059 ± 0.002[h]	0.385	0.619	0	0.340	0.742	0.302

[a] All data in THF at 30 °C.
[b] For 4 μm particle size columns. Values in parentheses correspond to nominal pore size of column packing material. See text for details.
[c] For all porosities, standard deviation < 0.001.
[d] Calculated using Eq. (8).
[e] Calculated using Eq. (10).
[f] Calculated using Eq. (9). Values of PSs on 4 μm particle size, 50 Å pore size column are zero because these analytes elute (or would elute, in the case of PS 19,760) at V_o, the total exclusion volume.
[g] These values are γ_t^{theor}, calculated according to Eq. (7) using γ_e, ε_e, and ε_t data from Table 1. See text for details.
[h] From Ref. [4].
[i] Values based on the assumption that PS 19,760 is expected to elute at the total exclusion volume of the 4 μm particle size, 50 Å pore size column.

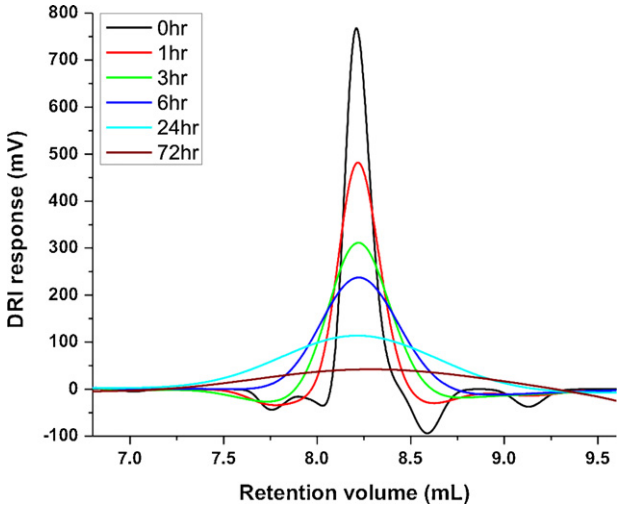

Fig. 2. Overlay of stop-flow chromatograms of toluene in 4 μm particle size, 50 Å pore size column. Solvent: THF, temperature: 30 °C. Baseline fluctuations are due to toluene eluting at the total permeation volume of the column (coelution with solvent has a negligible effect on peak height and width, however, as seen in the 24 h trace of Fig. 1, where toluene was not added). Baselines were drawn based on baseline away from peak, noting that baseline drift across chromatogram was negligible, in most cases «0.1 mV.

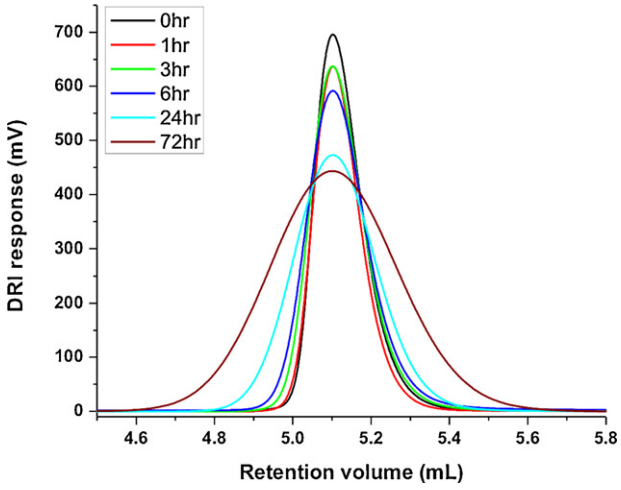

Fig. 3. Overlay of stop-flow chromatograms of PS 8450 in 4 μm particle size, 50 Å pore size column. Solvent: THF, temperature: 30 °C.

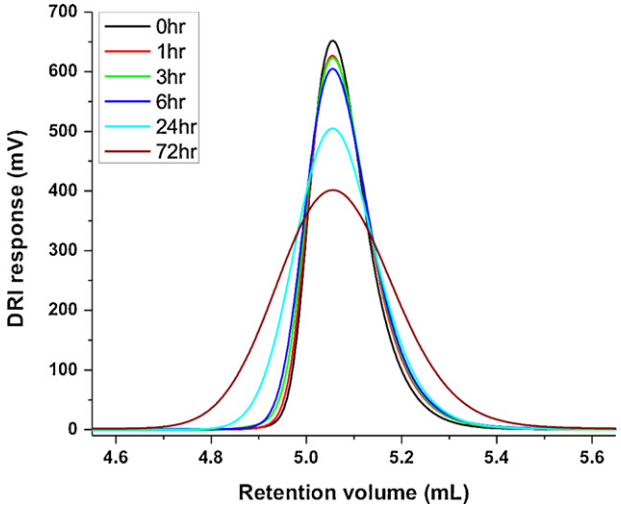

Fig. 4. Overlay of stop-flow chromatograms of PS 31,420 in 4 μm particle size, 50 Å pore size column. Solvent: THF, temperature: 30 °C.

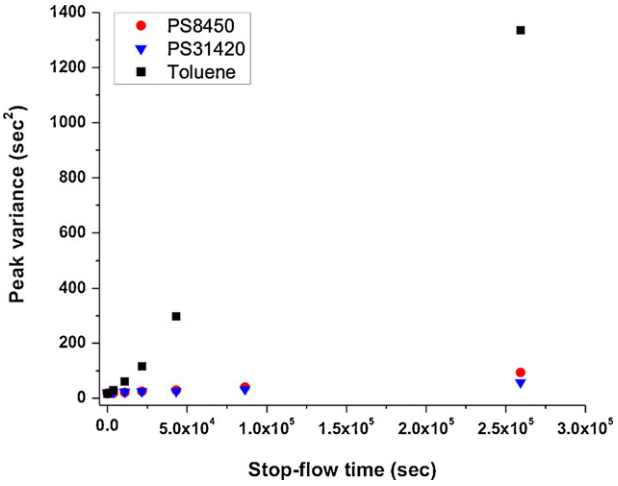

Fig. 5. Peak variance versus stop flow time for analytes on 4 μm particle size, 50 Å pore size column. Solvent: THF, temperature: 30 °C.

For the analytes studied here, the change in size (and, consequently, in D_m) over the 5 °C range of the conversion being effected employing Eq. (5) is, at best, minimal. The conversion was performed, nevertheless, to increase the accuracy of the results presented.

Based on the results shown in Figs. 1–6 and Table 1, Eq. (3) was used to calculate either γ_e (for nonpermeating analytes, for which $K_{SEC} = 0$) or γ_t (for permeating analytes, for which $K_{SEC} > 0$), with linear flow velocity ν calculated via:

$$\nu = \frac{uL}{V_R} \tag{6}$$

where u is the volumetric flow rate, L is the column length, and V_R is the retention volume of the analyte. For all PS analytes studied here, the 50 Å pore size column can be considered non-porous, as all these polymers are substantially larger than the pore size of the column packing material and, therefore, do not permeate into the pores (i.e., when using the 50 Å pore size column, $K_{SEC} = 0$ for all PS studied, as the latter elute at the total exclusion volume of the column). This is not the case for toluene, however, which did permeate into the pores of the packing material of both the 50 Å and the 10^4 Å columns.

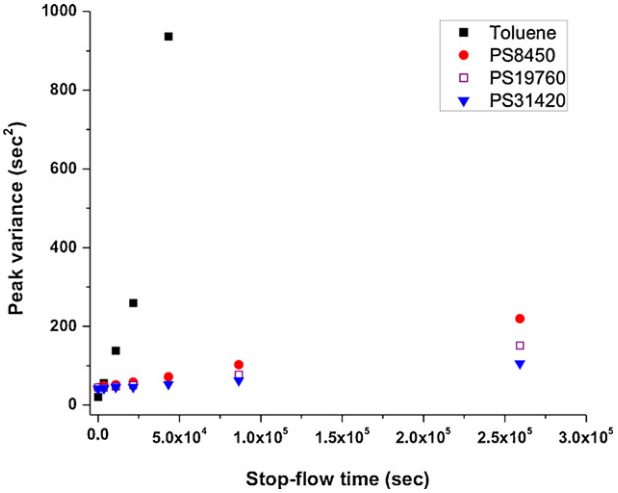

Fig. 6. Peak variance versus stop flow time for analytes on 4 μm particle size, 10^4 Å pore size column. Solvent: THF, temperature: 30 °C.

3.1. Relationship between γ_e, γ_p, and γ_t, and extension to hydrodynamic chromatography

Gritti and Guiochon have employed a mass balance approach to derive the equation for the apparent diffusion coefficient of an analyte in a packed porous medium in the absence of enthalpic interactions (i.e., when $\gamma_s = 0$) [12,14]. Here, we have used that equation as the basis through which to establish a relation between the interparticle, intraparticle, and total obstruction factors in SEC, in the form of Eq. (7):

$$\gamma_{t,SEC}^{theor} = \left(\frac{\varepsilon_e}{\varepsilon_t}\right)\gamma_e + \left(\frac{1-\varepsilon_e}{\varepsilon_t}\right)(K_D\varepsilon_p)\gamma_p \quad (7)$$

In this equation, ε_e, ε_p, and ε_t are the interparticle, intraparticle, and total column porosities, respectively, each defined as per [12]:

$$\varepsilon_e = \frac{V_o}{V_C} \quad (8)$$

$$\varepsilon_p = \frac{V_R - V_o}{V_c - V_o} \quad (9)$$

$$\varepsilon_t = \frac{V_M}{V_C} \quad (10)$$

where V_o is the total exclusion volume of the column, V_C is the total column volume (i.e., the volume of the empty column tube), V_R is the retention volume of the analyte, and V_M is the total permeating (void) volume of the column. According to Gritti and Guiochon, K_D is an enhanced drag coefficient meant to account for hydrodynamic resistance to diffusion in a porous material [14]. For a homologous series at a given set of experimental condition, the value $\gamma_p K_D$ is expected to decrease with increasing M. The difference between γ_t^{theor} and the γ_t determined using the stop-flow approach and Eq. (3) stems from the explicit inclusion of K_D and of the various ε factors in the calculation of γ_t^{theor}, whereas γ_t depends only on γ_e and γ_p in a manner that is currently undefined but which is likely to be additive. For the PSs in the 10^4 Å column, assuming a γ_e of 0.71 (based on the γ_e obtained for the 50 Å column) and a K_D of 0.5 (a crude approximation based on the K_D value of ≈0.71 for ethylbenzene in an 80 Å pore, as estimated by Gritti and Guiochon [14]), and employing the γ_p and ε values in Table 1, $\gamma_t^{theor} \approx 0.34$ are obtained, in reasonable agreement with the γ_t^{theor} of ≈0.44 calculated for PS 8450 and PS 31,420 in the 50 Å column using the data in Table 1, namely the γ_e obtained via the stop-flow approach and the porosities ε_e and ε_t of the 50 Å column (for these PSs in the 50 Å column, $\gamma_p = 0$).

In Eq. (7), for a given column the first term on the right hand side, $(\varepsilon_e/\varepsilon_t)\gamma_e$, will be essentially constant, as will be the $(1-\varepsilon_e)/\varepsilon_t$ modifier of γ_p. The importance of choosing an SEC column with both appropriate porosity and pore size for the purpose of minimizing band broadening in the analysis of a given polymer or set of polymers now becomes obvious, through the influence of the these parameters on γ_t, explicitly via the ε_p term and, implicitly, via γ_p.

For a technique such as packed-column hydrodynamic chromatography (HDC), which is currently experiencing a resurgence for the characterization of both polymers and particles [23,24], the second term on the right-hand side of Eq. (7) vanishes (because either non-porous column packings are used in HDC, or packings with small pores that cannot be accessed by large analytes, $\gamma_p = \varepsilon_p = 0$). In the absence of enthalpic interactions (i.e., with $\gamma_s = 0$), the analyte experiences only interparticle obstruction in HDC and Eq. (7) reduces to:

$$\gamma_{t,HDC}^{theor} = \left(\frac{\varepsilon_e}{\varepsilon_t}\right)\gamma_e \quad (11)$$

The γ_e term, which is essentially constant in SEC, is not necessarily so in HDC, either when using large-diameter column packing materials to analyze broadly disperse samples which include submicron-size particles [25,26] or when using columns packed with very small (e.g., sub-2 μm) particles to analyze broadly disperse samples which include large, ultra-high-M polymers [27]. In both these cases, the size of the polymer is a substantial fraction of the interstitial space (hydraulic radius, r_c; see Eq. (13) and accompanying discussion) and, for broadly disperse material, the γ_e of the material at one end of the size distribution may be significantly different from that of material at the opposite end of the distribution.

3.2. Results from stop-flow and variable-flow-rate experiments

From the data in Table 1 and in the figures, the following observations were made and conclusions drawn:

1. The γ_t of toluene, of PS 8450, and of PS 31,420 are larger in the 10^4 Å pore size column than in the 50 Å pore size column. The γ_t of the two PSs in the 50 Å column were calculated using Eq. (7) with $\gamma_p = 0$ (i.e., they are, technically, γ_t^{theor}; see Section 3.1). This is because, for these PSs in this column, the stop-flow experiments determine γ_e whereas, for toluene, it is γ_t that is determined. Because all the analytes studied can access the pores of the 10^4 Å column, in this column stop-flow experiments determine the γ_t of these analytes.

   The interparticle space is similar for both columns (they are both packed with 4 μm particle size particles and, as can be seen in Table 1, the interparticle porosities ε_e of the two columns differ from one another by only ≈10%), which should correspond to similar γ_e in both columns. There is more intraparticle space (larger ε_p) in the 10^4 Å column, however, therefore less intraparticle obstruction to diffusion, corresponding to a larger γ_p in the 10^4 Å as compared to the 50 Å column. Because, as shown above (Section 3.1 and Eq. (7)), γ_t is a function of both γ_e and γ_p (as well as being a function of the various column porosities), the fact that γ_e are expected to be similar in both columns, that there is little difference in ε_e, and that γ_p and ε_p are larger in the 10^4 Å column corresponds to a larger γ_t in this column, as well. For toluene (an analyte for which ε_p can be measured in both columns), its γ_t is ≈45% larger in the 10^4 Å column. As seen in Table 1, toluene has ≈60% more intraparticle space available in this column, some of which is offset by the fact that it has ≈12% less interparticle space available.
2. The interparticle obstruction factors of PS 8,450 and PS 31,420 in the 50 Å column are very similar to each other and higher than the classic 0.6 value of Knox and McLaren. In this column, these are both nonpermeating analytes (except, perhaps, for the lowest-M portions of their MMDs, present in only trace amounts; as mentioned above, these PSs elute at the total exclusion volume of this column) for which $\gamma_p = 0$. While the two analytes do differ from each other in size, this difference is ~1.5 nm, the hydrodynamic radius (R_H) of PS 8450 being 3.1 nm and that of PS 31,420 being 4.6 nm. These R_H values were calculated by incorporating the temperature-corrected D_m values calculated using Eq. (4) into the equation for R_H [16,28]:

$$R_H = \frac{k_B T}{6\pi\eta_0 D_m} \quad (12)$$

where k_B is Boltzmann's constant, T is the absolute temperature, and η_0 is the viscosity of the solvent at temperature T. This small difference in analyte sizes is negligible when compared to the interparticle distance of ~1400 nm, based on calculation of the hydraulic radius r_c as per [29,30]:

$$r_c = \frac{d_p\varepsilon}{3(1-\varepsilon)} \quad (13)$$

Because the interparticle space is so much larger than the size of either analyte, the analytes experience essentially the same obstruction to flow in the interstitial medium and, consequently, the γ_e of both analytes are essentially equal to one another.

The values of γ_e for PS 8450 and for PS 31,420 are 0.710 and 0.717, respectively (Table 1). While higher than the classic 0.6 value of Knox and McLaren, these values are closer to more recent data, such as $\gamma_e = 0.74$ determined using both non-porous silica and silica monoliths [10,15] and to $\gamma_e = 0.72 \pm 0.01$ obtained using polymer monoliths [11].

3. Only a small difference in the γ_t of PS 8450 and PS 31,420 is observed in the 10^4 Å pore size column. As noted in point 2 above, both these analytes should have approximately the same γ_e as each other in this column (as was the case with these analytes in the 50 Å column) and their ε_e and ε_t are identical (Table 1). As determined in our earlier study employing variable flow rates, there is only a small difference in the γ_p of both these analytes, which is offset by a small difference, if the opposite direction, in their ε_p (see Table 1). Consequently, their γ_t show little difference, as well.
4. In the 10^4 Å pore size column, the γ_t of toluene is smaller than are the γ_t of any of the polystyrenes studied. Because $K_{SEC,toluene} > K_{SEC,PS}$, there will be a higher concentration of toluene than of PS inside the pores of the column packing material. This corresponds to a lower concentration of toluene than of PS in the interstitial medium, and to fewer toluene molecules experiencing interparticle obstruction while more toluene molecules experience intraparticle obstruction, relative to PS. Because $\gamma_e > \gamma_p$, this results in $\gamma_{t,toluene} < \gamma_{t,PS}$. As noted, however, the effect is slight (i.e., the standard deviation Gaussians for the γ_t of toluene and of the PSs show some overlap with the $\pm 1\sigma$ region).
5. In the 10^4 Å pore size column, the γ_t of PS 19,760 is larger than the γ_t of both PS 8450 and PS 31,420. The γ_e of all these analytes should be essentially the same in this column, and also their ε_e and ε_t. As noted in our earlier publication [4], however, $\gamma_p \propto K_{SEC}\sqrt{M}$, corresponding to a maximum in the relationship between γ_p and M for a given set of analytes under a given set of experimental conditions. It would appear that the γ_p of PS 19,760 is closer to said maximum than are the γ_p of the other two polystyrenes studied, which is corroborated by the γ_p results shown in Table 1 and determined by an independent method (i.e., as explained earlier, the γ_p were determined using variable flow rate experiments, whereas the γ_t were determined using stop-flow experiments). Consequently, the γ_t of PS 19,760 is larger than the γ_t of the other two polystyrenes, as well.
6. In the 10^4 Å column, the γ_p of PS 19,760 is larger than are the γ_p of PS 8450 and of PS 31,420. This is due to the maximum in the γ_p versus M relationship, as explained in point 5 above and, more fully, in Ref. [4].
7. The γ_e determined for PS 8450 and PS 31,420 in the 4 μm particle size, 50 Å pore size column (which, as mentioned above, can be considered as non-porous from the point-of-view of these analytes) are approximately 12–14 times greater than the γ_p determined for these same analytes in the 4 μm particle size, 10^4 Å pore size column. First, it should be noted that "50 Å" and "10^4 Å" are nominal (and highly unrealistic) pore sizes that are actually meant to denote the end-to-end, fully stretched size of the smallest PS that is totally excluded from the column pores. Secondly, we note that the exclusion limit (based on PS in THF at room temperature) of the 10^4 Å column is given by the manufacturer as 600,000 g mol^{-1}, but that our own experiments showed this exclusion limit to be somewhat higher than 1,100,000 g mol^{-1} [31]. The latter M corresponds to an R_G of approximately 50 nm [30,32], providing for a crude estimate of the pore diameter of approximately 100 nm. This pore diameter is ~14 times smaller than the interstitial diameter ($2r_c$) of this column, as calculated above using Eq. (13), showing good agreement between the magnitude of the obstruction factor and the size of the "container" within which diffusion is being obstructed.

4. Conclusions

We conclude here (at least for the time being) our investigation of the various column obstruction factors in size-exclusion chromatography. The venerable stop-flow method was employed to determine the interparticle (for analytes for which $K_{SEC} = 0$) or the total (for analytes for which $K_{SEC} > 0$) obstruction factor, γ_e and γ_t, respectively. In conjunction with the intraparticle obstruction factor γ_p determined using a variable-flow-rate approach and with column porosity measurements, these data provide insight into the relative contributions of the different factors to the longitudinal diffusion and stagnant mobile phase mass transfer terms of the van Deemter and related equations. Not considered here were the effects of the pore size and particle size distributions on the various γ terms. Because both columns contain the same type of packing material, and given the similarity in their interparticle porosities, the latter effects are assumed to be negligible or non-existent. While they are expected to be minor, differences in column pore size distributions (which are data not generally disclosed by column manufacturers), if present, could not be assessed.

Our calculated γ_p for SEC fall far below even the lowest value predicted by Giddings. The interparticle obstruction factor γ_e from the present experiments is 0.71–0.72, slightly above the classic 0.6 value of Knox and McLaren, but remarkably similar to more recently determined values for both non-porous packings and monoliths.

The recent work of Gritti and Guiochon was recast in terms of the interrelationship between the total, interparticle, and intraparticle obstruction factors and the various column porosities, for both size-exclusion and hydrodynamic chromatography. The importance of both column porosity and pore size in minimizing the stagnant mobile phase contribution to band broadening in SEC was demonstrated, as was the importance of particle size (vis-à-vis analyte size) for minimizing band broadening due to mass transfer between streamlines of flow in HDC.

Disclaimer

Commercial products are identified to specify adequately the experimental procedure. Such identification does not imply endorsement or recommendation by the National Institute of Standards and Technology, nor does it imply that the materials identified are necessarily the best available for the purpose.

References

[1] J.C. Giddings, Dynamics of Chromatography, Marcel Dekker, New York, 1965.
[2] J.H. Knox, L. McLaren, Anal. Chem. 36 (1964) 1477.
[3] S.J. Hawkes, Anal. Chem. 44 (1972) 1296.
[4] D.J. Richard, A.M. Striegel, J. Chromatogr. A 1217 (2010) 7131.
[5] J.H. Knox, H.P. Scott, J. Chromatogr. 282 (1983) 297.
[6] J.H. Knox, J. Chromatogr. A 831 (1999) 3.
[7] J.H. Knox, J. Chromatogr. A 960 (2002) 7.
[8] S.J. Hawkes, S.P. Steed, J. Chromatogr. Sci. 8 (1970) 256.
[9] J. Klein, M. Grüneberg, Macromolecules 14 (1981) 1411.
[10] K. Miyabe, J. Chromatogr. Sci. 47 (2009) 452.
[11] G.W. Anderson, Z. LaPier, T.S. Cullum, M.M. Bushey, Electrophoresis 31 (2010) 1583.
[12] F. Gritti, G. Guiochon, Chem. Eng. Sci. 61 (2006) 7636.
[13] K. Miyabe, Y. Matsumoto, G. Guiochon, Anal. Chem. 79 (2007) 1970.
[14] F. Gritti, G. Guiochon, Anal. Chem. 79 (2007) 3188.
[15] K. Miyabe, N. Ando, G. Guiochon, J. Chromatogr. A 1216 (2009) 4377.
[16] A.M. Striegel, W.W. Yau, J.J. Kirkland, D.D. Bly, Modern Size-Exclusion Liquid Chromatography, 2nd ed., Wiley, New York, 2009.

[17] A.M. Striegel, J. Chromatogr. A 932 (2001) 21.
[18] A.M. Striegel, J. Am. Chem. Soc. 125 (2003) 4146 (see Erratum in J. Am. Chem. Soc. 126 (2004) 4740).
[19] T.D. Buley, A.M. Striegel, Carbohydr. Polym. 79 (2010) 241.
[20] A.M. Striegel, M.A. Boone, Biopolymers 95 (2011) 228.
[21] V. Wernert, R. Bouchet, R. Denoyel, Anal. Chem. 82 (2010) 2668.
[22] A. Berthod, F. Chartier, J.-L. Rocca, J. Chromatogr. 469 (1989) 53.
[23] A.M. Striegel, Anal. Bioanal. Chem. 402 (2012) 77.
[24] A.M. Striegel, A.K. Brewer, Ann. Rev. Anal. Chem 5 (2012) 15.
[25] A.K. Brewer, A.M. Striegel, Anal. Bioanal. Chem. 393 (2009) 295.
[26] A.K. Brewer, A.M. Striegel, J. Sep. Sci. 33 (2010) 3555.
[27] E. Uliyanchenko, S. van der Wal, P.J. Schoenmakers, J. Chromatogr. A 1218 (2011) 6930.
[28] M.J. Smith, I.A. Haidar, A.M. Striegel, Analyst 132 (2007) 455.
[29] A.M. Striegel, J. Liq. Chromatogr. Relat. Technol. 31 (2008) 3105.
[30] A.M. Striegel, S.L. Isenberg, G.L. Côté, Anal. Bioanal. Chem. 394 (2009) 1887.
[31] A.M. Striegel, J. Chromatogr. A 1033 (2004) 241.
[32] M.E. van Kreveld, N. van den Hoed, J. Chromatogr. 83 (1973) 111.